# Relation between tidal damping and wave celerity in estuaries

Hubert H. G. Savenije[1] and Ed J. M. Veling
Delft University of Technology, Delft, Netherlands

Received 13 January 2004; revised 27 January 2005; accepted 11 February 2005; published 21 April 2005.

[1] Observations in estuaries indicate that an amplified tidal wave moves considerably faster than is indicated by the classical equation for wave propagation. Similarly, the celerity of propagation is lower if the tidal wave is damped. This phenomenon is clearly observed in the Schelde estuary (located in the Netherlands and Belgium) and in the Incomati estuary in Mozambique. In the Incomati, the tidal wave is damped throughout, whereas in the Schelde the tidal range increases from the mouth until the city of Antwerp, after which it decreases until Gent. This paper derives a new analytical expression for the celerity of the tidal wave that takes into account the effect of tidal damping, as an expansion of the classical equation for tidal wave propagation. In the new equation the phase lag between high water and high water slack plays a crucial role. It is one of the main parameters determining tidal wave propagation in alluvial estuaries. The equation is successfully applied to observations in the Schelde and the Incomati.

**Citation:** Savenije, H. H. G., and E. J. M. Veling (2005), Relation between tidal damping and wave celerity in estuaries, *J. Geophys. Res.*, *110*, C04007, doi:10.1029/2004JC002278.

## 1. Introduction

[2] The classical formula for wave propagation is widely used to describe the propagation of a tidal wave in estuaries. This equation has been derived for the propagation of a small amplitude gravity wave in a channel of constant cross section with no friction or bottom slope,

$$(c_0 - v)^2 = \frac{1}{\beta} gh, \tag{1}$$

where $c_0$ is the classical celerity of the wave (m/s), $g$ is the acceleration due to gravity (m/s$^2$), $v$ is the stream velocity averaged over the cross section, $h$ is the stream depth averaged over the cross section, and $\beta$ is a coefficient that accounts for storage outside the stream section of the channel ($\beta > 1$). Under these conditions, the water level and flow are in phase.

[3] The fact that this equation is so widely used in estuaries is surprising since the conditions for its derivation (constant cross section and no friction) do not apply in alluvial estuaries where the cross section varies exponentially along the estuary axis and friction is clearly not negligible. It will be demonstrated that the classical wave equation also describes the propagation of a tidal wave in a converging channel (albeit with a phase lag $\varepsilon$ ($0 < \varepsilon < \pi/2$) between high water and high water slack), as long as it does not gain or lose amplitude as it travels upstream and the energy per unit width, that is present in the wave, is constant. This is the case when the energy gain as a result of the convergence of the banks, as the wave travels upstream, is compensated by the energy lost by friction. In this situation one speaks of an "ideal estuary" [*Pillsbury*, 1939], leading to an estuary of constant depth, an exponentially varying width, a constant wave celerity, and a constant phase lag between water level and velocity. The exponential width variation has been used widely to derive analytical equations for tidal wave propagation [see, e.g., *Hunt*, 1964; *Harleman*, 1966; *Jay*, 1991; *Savenije*, 1992; *Friedrichs and Aubrey*, 1994; *Lanzoni and Seminara*, 1998, 2002]. If the effect of convergence is stronger than the effect of friction, then the wave is amplified; when the friction is stronger than the effect of convergence, the wave is damped. An analytical equation demonstrating this effect was derived by *Savenije* [1998, 2001], and is reproduced farther down (see equation (34)). Although in an ideal estuary there is no tidal damping or amplification, in real estuaries there generally is, albeit modest. The length scale of tidal damping is generally large in relation to the length scale of bank convergence [see, e.g., *Friedrichs and Aubrey*, 1994; *Savenije*, 1992].

[4] There appears to be a close relation between tidal damping (or amplification) and wave celerity. Tidal damping and tidal wave celerity both react to the imbalance between convergence and friction. In estuaries where tidal damping or amplification is apparent (e.g. the Thames, the Schelde, or the Incomati; see Figure 1), one can observe a prominent deviation from the classical wave celerity $c_0$. If the wave is amplified, such as in the lower parts of the Thames and the Schelde, then the wave moves considerably faster than the celerity computed by equation (1); when the wave is damped, as is the case in the Incomati and in upper parts of the Thames and Schelde, then the wave travels considerably slower.

[5] Observations of tidal wave celerity under tidal damping and amplification are presented in Figure 2 for the

[1] Also at UNESCO Institute for Water Education (IHE), Delft, Netherlands.


0148-0227/05/2004JC002278$09.00

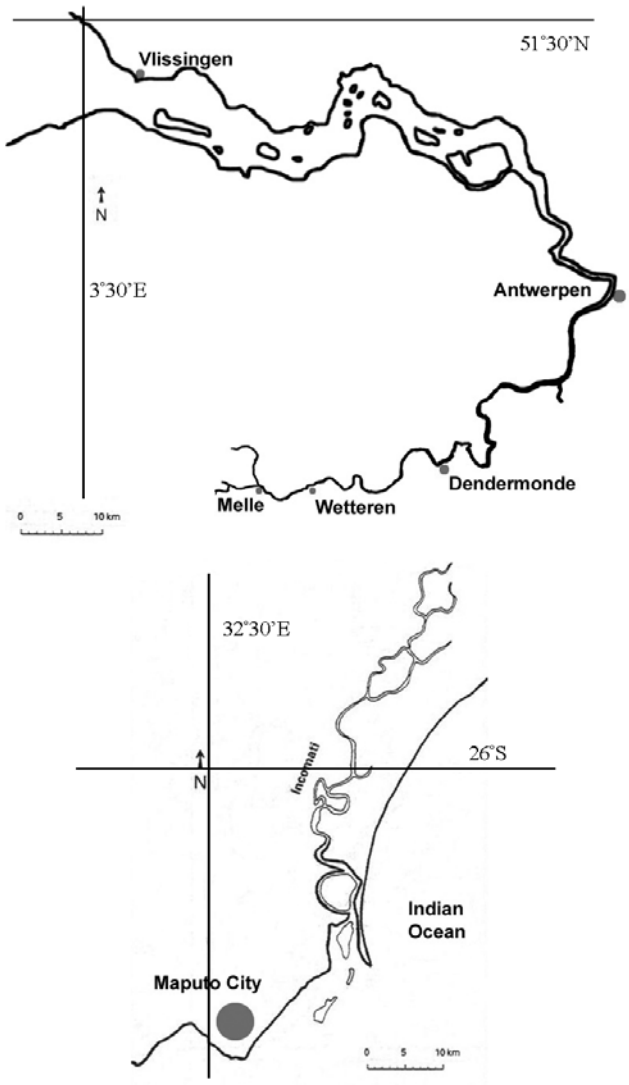


**Figure 1.** (top) Schelde estuary. (bottom) Incomati estuary. See color version of this figure in the HTML.

Schelde in Netherlands and the Incomati in Mozambique. These observations are combined with a drawn line representing the classical equation for wave propagation of equation (1). Figure 2 shows observations at high water (HW) and low water (LW) in the Schelde and observations at high water slack (HWS) and low water slack (LWS) in the Incomati. It can be seen clearly that in an amplified estuary (the lower Schelde) the travel time of the wave is much shorter than the travel time computed by equation (1) (about half) and that the travel time is substantially larger in a damped estuary (the upper Schelde and the Incomati).

[6] To date, the analysis of finite amplitude effects in convergent, frictional estuaries has been little explored. *Ponce and Simons* [1977] remarked that "a coherent theory that accounts for celerity as well as attenuation characteristics has yet to be formulated." *Godin* [1991, 1999] analyzed the nonlinear effects of river discharge and friction, but did not come up with a revised expression for the wave celerity. To date, the most substantial contributions made to solving this problem are by *Jay* [1991] and by *Friedrichs and Aubrey* [1994], who addressed it by scaling the governing equations and subsequently solving the first- and second-order approximations analytically. This approach, which is also called the perturbation approach, reduces the differential equation by neglecting higher order terms. In doing so, the effect of tidal damping generally disappears from the equation. Only in a second-order solution are the combined effects of tidal damping and wave propagation present. *Friedrichs and Aubrey* [1994] fitted their equations to observations in the Thames, Tamar, and Delaware by calibration. Although the method was based on the linearized Saint Venant equations, they were able to demonstrate a combined effect of damping/amplification and wave celerity, by retaining an exponentially decaying or increasing tidal amplitude.

[7] In this paper, the method of characteristics [see, e.g., *Dronkers*, 1964; *Whitham*, 1974] is used to derive an analytical equation for the combined effect of damping and wave celerity. This equation allows the computation of the celerity of propagation under damped or amplified conditions. The equation obtained is not very complicated and is an extension of the classical formula, in which besides the rate of amplification (or damping), the phase lag $\varepsilon$ between high water and high water slack is essential.

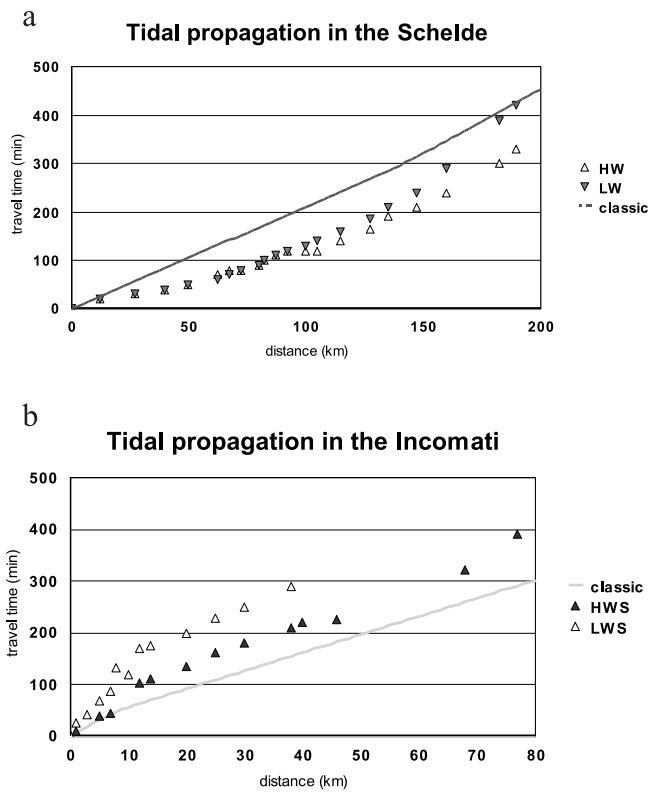


**Figure 2.** (a) Observed propagation of the tidal wave at HW and LW on 21 June 1995 in the Schelde, compared to the propagation computed with the classical equation (equation (1)). (b) Observed propagation of the tidal wave at HWS and LWS on 23 June 1993 in the Incomati, compared to the propagation computed with the classical equation (equation (1)). See color version of this figure in the HTML.

The inclusion of $\varepsilon$ is crucial in the methodology. It is one of the most important parameters characterizing tidal hydraulics in estuaries. Conditions for the derivations made are that the tidal amplitude to depth ratio and the Froude number are considerably smaller than unity and that the velocity of river discharge is small compared to the tidal velocity. In the lower part of alluvial estuaries this situation is the rule rather than the exception.

## 2. Theory

[8] The following one-dimensional equations determine the water level and flow velocity fluctuations of the water in a well-mixed estuary:

$$\frac{\partial A}{\partial t} + \frac{\partial Q}{\partial x} = 0 \tag{2}$$

$$\frac{\partial v}{\partial t} + v\frac{\partial v}{\partial x} + g\frac{\partial h}{\partial x} + g\frac{\partial z_b}{\partial x} + \frac{gh}{2\rho}\frac{\partial \rho}{\partial x} + \frac{fv|v|}{h} = 0, \tag{3}$$

where $A(x,t)$ is the cross-sectional area of the estuary, $Q(x,t)$ is the discharge, $v(x,t)$ is the velocity of flow, $h(x,t)$ is the depth of flow, $z_b(x)$ is the bottom level, $\rho$ is the density of the water, and $f$ is a roughness coefficient. Most of the flow parameters are functions of both distance $x$ and time $t$. The positive $x$-direction is chosen upstream with the origin at the estuary mouth.

[9] These are the Saint Venant equations, where the first equation accounts for conservation of mass and the second for conservation of momentum. In addition, the following geometric equations apply to $A$ and $Q$:

$$A = hB_s \tag{4}$$

$$Q = hBv, \tag{5}$$

where $B(x)$ is the stream width and $B_s(x)$ is the storage width, which may be larger than the stream width $B$, particularly at high water levels.

[10] In alluvial estuaries, the stream width of the estuary at a particular water level, for example, at HW, LW, or tidal average (TA), can generally be described by an exponential function.

$$B = B_0 \exp\left(-\frac{x}{b}\right). \tag{6}$$

The length scale of the exponential function is a constant: $b$, which is named the convergence length.

[11] A useful equation was derived by *Savenije* [1993] from the water balance equation relating the tidal amplitude to tidal velocity amplitude,

$$\frac{\eta}{\upsilon} = \frac{\overline{h}(1-\delta_u b)}{\omega b \cos\varepsilon}, \tag{7}$$

where $\eta$ is the tidal amplitude equal to half the tidal range $H$, $\overline{h}$ is the time-average depth, $\upsilon$ is the amplitude of the tidal velocity, $\omega = 2\pi/T$ is the angular velocity, $\varepsilon$ is the phase lag between high water (HW) and high water slack (HWS), and $\delta_u$ is the damping scale of the tidal velocity defined by

$$\delta_u = \frac{1}{\upsilon}\frac{d\upsilon}{dx}. \tag{8}$$

[12] If damping is modest and the depth and phase lag are constant along the estuary axis, which is generally the case in alluvial estuaries, than it follows from (7) that the damping of the tidal velocity amplitude equals the damping of the tidal range, defined by

$$\delta_H = \frac{1}{H}\frac{\mathrm{d}H}{\mathrm{d}x} = \frac{1}{\eta}\frac{\mathrm{d}\eta}{\mathrm{d}x}. \tag{9}$$

[13] Combination of (6) with the Saint Venant equations and some elaboration yields

$$\beta\frac{\partial h}{\partial t} + h\frac{\partial v}{\partial x} + v\frac{\partial h}{\partial x} - \frac{vh}{b} = 0 \tag{10}$$

$$\frac{\partial v}{\partial t} + v\frac{\partial v}{\partial x} + g\frac{\partial h}{\partial x} + gI_b - gI_r + \frac{fv|v|}{h} = 0, \tag{11}$$

where $\beta = B_s/B > 1$ is the storage width correction factor, $I_b$ is the bottom slope, $I_r$ is the density slope (in agreement with the fourth and fifth terms, respectively, of equation (3)). If the salinity of the seawater is 1024 kg/m$^3$, then the density slope amounts to about $0.12h/L$, where $L$ is the intrusion length of the salinity in the estuary. In the Schelde this slope results in an increase of the water level at Antwerp of almost 0.2 m. At the downstream boundary a periodic water level fluctuation is assumed, and at the upstream boundary a river discharge $Q_r$, which should be small compared to the tidal flow.

[14] If we assume that topographic parameters such as $\beta$, $b$, and $I_b$ can be determined independently, then the two equations have three unknowns: $h$, $v$, and $f$. The latter is generally obtained from calibration on measurements. The main unknown parameters to be determined in the analysis, as functions of time and space, are the water depth and the water velocity. Both are considered periodic functions $\Phi$ and $\Psi$, with a tidal period $T$ and an angular velocity $\omega = 2\pi/T$.

[15] Hence the assumed shape of the periodic functions for velocity and depth are

$$v = \upsilon\Phi(\xi - \varepsilon), \tag{12}$$

$$h = \eta\Psi(\xi) + \overline{h}, \tag{13}$$

$$\xi = \omega\left(t - \frac{x}{c}\right), \tag{14}$$

where $\upsilon(x)$ is the amplitude of the tidal velocity, $\eta(x)$ is the amplitude of the tidal water level variation ($\eta = H/2$), $\overline{h}$ is the tidal average depth, $\xi$ is the dimensionless argument of the periodic function, $c$ is the celerity of the tidal wave, and $\varepsilon$ is the phase lag between high water (HW) and high water slack (HWS), or between low water (LW) and low water

slack (LWS), which, in agreement with the ideal estuary, can be assumed to be constant along the estuary axis [e.g., *Lanzoni and Seminara*, 2002], if the tidal amplitude to depth ratio and the river discharge is small compared to the tidal flow. We shall assume that we know the shape of the harmonics $\Phi$ and $\Psi$ (sinusoids); the two main variables $h$ and $v$ then are replaced by the variables $\upsilon(x)$ and $\eta(x)$. Assuming the average depth can be derived from topography, there are only two more variables introduced: $\varepsilon$ and $c$. The solution of the Saint Venant equations will thus require two more equations. One of the equations is (7), and the other is an expression for the phase lag derived by *Savenije* [1993] from the conservation of mass equation,

$$\tan\varepsilon = \frac{\omega b}{(1-\delta_u b)c}. \tag{15}$$

[16] This expression is similar to the one derived by *Prandle* [2003]. Combination of this equation with (7) yields the "Scaling equation"

$$\frac{\upsilon}{c} = \beta\frac{\eta\sin\varepsilon}{\overline{h}}. \tag{16}$$

This "Scaling equation" corresponds with its classical counterpart when $\sin\varepsilon = 1$: the case of a progressive wave [e.g., *Jay*, 1991, equation (6); *Friedrichs and Aubrey*, 1994, equation (11)].

[17] Thus we have four equations with (besides $f$) four unknowns. The damping scales for tidal range and velocity are not additional variables, since they are defined by (8) and (9). The added value of this approach is that the tidal damping, the wave celerity, and the phase lag can all be determined directly from observations, so that an estimate of the roughness and, for instance, the average depth can be made analytically.

[18] Hence the following conditions should be met:

[19] 1. The tidal velocity $v$ in (11) is not influenced significantly by the river discharge $Q_r$. Hence $\upsilon \gg Q_r/A$.

[20] 2. The amplitude of the tidal water level variation is smaller than the depth of flow. Hence $\eta < h$.

[21] 3. The Froude number is small: $\upsilon \ll c$.

[22] 4. The phase lag $\varepsilon$ is constant along the estuary.

[23] 5. The wave celerity is constant along the estuary, or at least along a certain reach of the estuary, or $\partial c/\partial x = 0$.

[24] 6. The scaled tidal wave ($\Psi$) is not deformed as it travels upstream.

[25] The first assumption is very common in tidal hydraulics and quite acceptable in the downstream part of alluvial estuaries. The second is only correct in deep estuaries. In a shallow estuary such as the Incomati (see Figure 1) this situation does not apply near the estuary mouth, although it does farther upstream. Assumption 3 is linked to the second assumption through the scaling equation (16). With $\beta\sin\varepsilon$ being smaller than unity in alluvial estuaries, the Froude number is always smaller than the tidal amplitude to depth ratio. Assumption 4 corresponds to the theory of the ideal estuary, which in alluvial estuaries is a good approximation of reality. The fifth assumption is crucial for the derivations made. It is also in agreement with the theory of the ideal estuary. Its validity shall be checked in section 3 for the estuaries studied. Assumption 6, finally, is the methodological assumption. This assumption, which implies that higher order effects are negligible, is less restrictive than the assumption made for the derivation of the classical equation. Assumption 6 is acceptable as long as assumptions 1–3 are valid, and hence it is not really an additional assumption.

[26] The following partial derivatives can be derived for the parameters of the harmonic functions:

$$\frac{\partial\xi}{\partial t} = \omega \tag{17}$$

$$\frac{\partial\xi}{\partial x} = -\frac{\omega}{c}. \tag{18}$$

The average water depth gradient can be found by averaging (11) over time, under the assumption that the residual effect of the friction term is small. This is only correct under the strict assumptions of a small tidal range to depth ratio, a small Froude number, and negligible river flow. *Horrevoets et al.* [2004] demonstrated that this is acceptable in the part of the estuary where river discharge is small compared to tidal flow (assumption 1). Hence

$$\frac{\partial\overline{h}}{\partial x} = I_r - I_b. \tag{19}$$

Subsequently, the following partial derivatives of velocity and depth can be written:

$$\frac{\partial v}{\partial t} = \upsilon\Phi'\frac{\partial\xi}{\partial t} = \upsilon\omega\Phi', \tag{20}$$

$$\frac{\partial v}{\partial x} = \upsilon\Phi'\frac{\partial\xi}{\partial x} + \Phi\frac{\partial\upsilon}{\partial x} = -\frac{\upsilon}{c}\omega\Phi' + \upsilon\delta_u\Phi, \tag{21}$$

$$\frac{\partial h}{\partial t} = \eta\Psi'\frac{\partial\xi}{\partial t} = \eta\omega\Psi', \tag{22}$$

$$\frac{\partial h}{\partial x} = \eta\Psi'\frac{\partial\xi}{\partial x} + \Psi\frac{\partial\eta}{\partial x} + \frac{\partial\overline{h}}{\partial x} = -\eta\frac{\omega}{c}\Psi' + \eta\delta_H\Psi + I_r - I_b. \tag{23}$$

Note that for these derivatives it is not necessary to assume that the periodic functions are simple harmonics.

[27] Essential for the further derivation is the assumption that the wave may be amplified or damped, but that the scaled tidal wave ($\Psi$) is not deformed, as long as the observer travels along a characteristic at the wave celerity ($\Psi$ is constant with time if $\xi$ is constant with time, implying that $dx/dt = c$). As we can see from Figure 3, showing the propagation of tidal waves in the Schelde estuary, the tide has a higher order $M_4$ component resulting from the nonlinear resistance term. The shape of the scaled tidal wave, however, remains similar as the wave travels upstream. In the following, we assume a sinus shape.

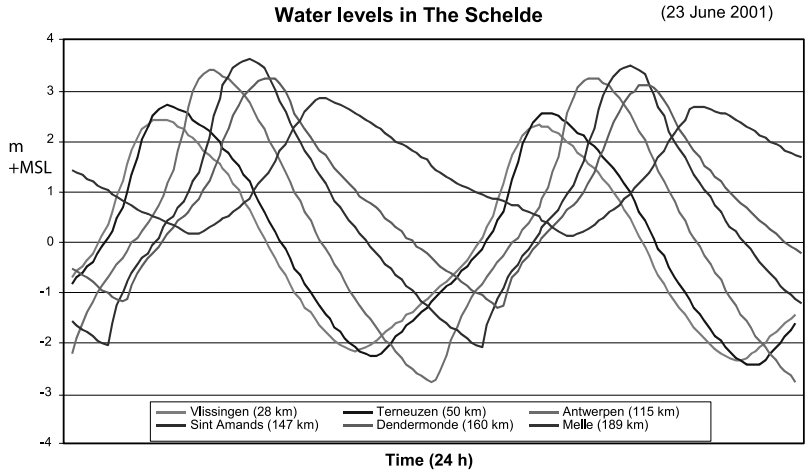


**Figure 3.** Observed tidal waves at different points along the Schelde estuary on 23 June 2001. See color version of this figure in the HTML.

[28] Hence, for an observer traveling at the celerity of the tidal wave,

$$\frac{d\Psi(x,t)}{dt} = \frac{\partial \Psi}{\partial t} + c\frac{\partial \Psi}{\partial x} = \frac{\partial \Psi}{\partial \xi}\frac{\partial \xi}{\partial t} + c\frac{\partial \Psi}{\partial \xi}\frac{\partial \xi}{\partial x} = \Psi'\left(\frac{\partial \xi}{\partial t} + c\frac{\partial \xi}{\partial x}\right) = 0. \quad (24)$$

The crux of the method is that application of equation (24) to the combined Saint Venant equations implies that the sum of all terms containing $\Psi'$ should be zero. These terms should be found in a linear combination of the two equations. Thus the equation of continuity (7) is multiplied by a constant factor $m$ and added to the equation of motion (8), after which the sum of all terms containing $\Psi'$ are equated to zero. Such a method is more often used to determine the celerity of propagation, for example by *Sobey* [2001], who applied it to a channel of constant cross section and disregarded the effect of tidal damping. As a result, our approach generates more terms.

[29] To enhance insight into the terms of the Saint Venant equations, they are represented in Table 1 in a format where each column lists the coefficients of the equations belonging to the variables $\Psi'$, $\Phi'$, $\Psi$, and $\Phi$ for each term of the equations. In this table there are a number of cells that contain non-linear terms. These terms could also have been placed in another column. The reason why a certain column is chosen is to provide a logical overview. The position of these terms is not affecting the further analysis. What is essential for the following analysis is to see which terms belong to $\Psi'$.

[30] The combined equation can be split into two parts: the equation where the sum of the coefficients of the terms containing $\Psi'$ is zero (corresponding to equation (24)) and the equation where the sum of the remaining terms is zero. The first equation yields

$$m\left(\beta\eta\omega - v\frac{\omega}{c}\eta\right) = g\frac{\omega}{c}\eta$$

or

$$m = \frac{g}{(c\beta - v)}, \quad (25)$$

where $m$ is the multiplication factor for the equation of continuity.

[31] The second equation reads

$$m\left\{-h\frac{\upsilon\omega}{c}\Phi' - \upsilon h\left(\frac{1}{b} - \delta_u\right)\Phi + \upsilon\Phi(\eta\delta_H\Psi + I_r - I_b)\right\} + \upsilon\omega\left(1 - \frac{v}{c}\right)\Phi' + g\eta\delta_H\Psi + \left(\frac{f\upsilon|v|}{h} + v\upsilon\delta_u\right)\Phi = 0. \quad (26)$$

Substitution of $m$ and rearrangement yields

$$(c\beta - v)(c - v) = gh\frac{1 + C + S + D_2 + D_3}{1 - (R + D_1 + D_4)(c/(c - v))} = ghF, \quad (27)$$

with $F$ being a function of $\Phi$ and $\Psi$, consisting of the following terms:

$$C = \frac{\Phi c}{\Phi'\omega}\frac{1}{b},$$

$$S = \frac{\Phi c}{\Phi' h\omega}(I_b - I_r),$$

$$R = -\frac{\Phi}{\Phi'\omega}\frac{f|v|}{h},$$

$$D_1 = -\frac{g}{\Phi'\upsilon\omega}\eta\Psi\delta_H,$$

$$D_2 = -\frac{\Phi c}{\Phi'\omega}\delta_u,$$

$$D_3 = -\frac{\Phi c}{\Phi' h\omega}\eta\Psi\delta_H,$$

$$D_4 = -\frac{\Phi}{\Phi'\omega}\upsilon\Phi\delta_u.$$

[32] These terms are all functions of $v$ and $h$, and hence of time and space. Here $C$ is the term that determines the acceleration of the wave due to the convergence of the banks. $S$ determines the influence of the bottom slope; $R$ determines the effect of friction, and the $D_i$ terms ($i = 1, .., 4$) contain the effect of tidal amplification or damping. The

**Table 1.** Representation of the Terms of the Saint Venant Equations as Functions of $\Psi'$, $\Phi'$, $\Psi$, and $\Phi$

| Term | $\Psi'$ | $\Phi'$ | $\Psi$ | $\Phi$ | Constant |
|---|---|---|---|---|---|
| $\beta\frac{\partial h}{\partial t}$ | $\beta\eta\omega$ | ... | ... | ... | ... |
| $-\frac{vh}{b}$ | ... | ... | ... | $-\frac{\upsilon h}{b}$ | ... |
| $h\frac{\partial v}{\partial x}$ | ... | $-h\frac{\upsilon\omega}{c}$ | ... | $+h\upsilon\delta_u$ | ... |
| $v\frac{\partial h}{\partial x}$ | $-v\frac{\omega}{c}\eta$ | ... | $v\eta\delta_H$ | $-\upsilon(I_b - I_r)$ | ... |
| $\frac{\partial v}{\partial t}$ | ... | $\upsilon\omega$ | ... | ... | ... |
| $v\frac{\partial v}{\partial x}$ | ... | $-v\frac{\upsilon\omega}{c}$ | ... | $+v\upsilon\delta_u$ | ... |
| $g\frac{\partial h}{\partial x}$ | $-g\frac{\omega}{c}\eta$ | ... | $g\eta\delta_H$ | ... | $-g(I_b - I_r)$ |
| $g(I_b - I_r)$ | ... | ... | ... | ... | $g(I_b - I_r)$ |
| $\frac{fv\lvert v\rvert}{h}$ | ... | ... | ... | $\frac{f\upsilon\lvert v\rvert}{h}$ | ... |

terms are defined such that if they are positive, they cause the wave to move faster; if they are negative, they slow down the propagation of the wave. Because in alluvial estuaries the Froude number is much smaller than unity, $|D_4| \ll |D_2|$ and $|D_3| \ll |D_1|$. As a result, $D_4$ and $D_3$ can generally be disregarded, but we retain them here.

[33] Besides that $F$ is a function of $v$ and $h$, equation (27) contains the flow velocity and the depth explicitly. This dependency on $v$ and $h$ can be simplified using an adjusted Airy equation. *Airy* [1845], quoted by *Lamb* [1932, article 175], presented the following equation for a frictionless undamped progressive wave ($\sin\varepsilon = \pi/2$) in a prismatic channel with no bottom slope:

$$c = \overline{c_0}\left(1 + \frac{3\eta}{2\overline{h}}\right), \tag{28}$$

where $\overline{c_0}$ is the classical celerity of the tidal wave at mean depth. In our case, where there is friction, tidal damping, and a strong topography, this equation is different. For a small Froude number, equation (27) can be modified as

$$(c - v)^2 = \overline{c_0}^2\left(1 + \frac{h - \overline{h}}{\overline{h}}\right)F. \tag{29}$$

[34] Let us consider the situation at HW. At HW: $h - \overline{h} = \eta$ and $v = \upsilon\sin\varepsilon$. Making use of the scaling equation (16), this leads to

$$c_{HW} = \overline{c_0}\left(1 + \frac{\eta}{\overline{h}}\right)^{0.5} F_{HW}^{0.5} + \overline{c_0}\beta\frac{\eta}{\overline{h}}\sin^2\varepsilon. \tag{30}$$

[35] The root in the first term can be replaced by the first terms of a Taylor series expansion, if $\eta/h < 1$. Hence

$$\begin{aligned} c_{HW} &= \overline{c_0}\left(1 + \frac{\eta}{2\overline{h}}\right)F_{HW}^{0.5} + \overline{c_0}\beta\frac{\eta}{\overline{h}}\sin^2\varepsilon \\ &= \overline{c_0}\left(1 + \frac{\eta}{\overline{h}}\left(\frac{1}{2} + \beta\frac{\sin^2\varepsilon}{F_{HW}^{0.5}}\right)\right)F_{HW}^{0.5}. \end{aligned} \tag{31}$$

Now it can be seen that for $\beta = 1$, $F = 1$, and $\varepsilon = \pi/2$ (the case of an undamped progressive wave in a prismatic channel) this is the same as Airy's equation. In alluvial estuaries, however, the value of $\sin^2\varepsilon$ is O(0.1). With $F$ and $\beta$ being close to unity, this implies that in alluvial estuaries the effect of the wave amplitude on the wave celerity is less strong, as Airy's equation suggests. The general equation for the effect of depth and velocity variation on wave propagation can be derived similarly as

$$\begin{aligned} c &= \overline{c_0}\left(1 - \frac{\eta}{2\overline{h}}\Psi\right)F^{0.5} - \overline{c_0}\beta\frac{\eta}{\overline{h}}\Phi\sin\varepsilon \\ &= \overline{c_0}\left(1 - \frac{\eta}{\overline{h}}\left(\frac{\Psi}{2} + \beta\frac{\Phi\sin\varepsilon}{F^{0.5}}\right)\right)F^{0.5}. \end{aligned} \tag{32}$$

For a small amplitude-to-depth ratio, the direct effect of the water level fluctuation on the wave celerity is small. However, there is a stronger effect through $F$ that we have not yet explored.

[36] The values of $C$, $S$, $R$, and $D_i$ vary during the tidal cycle. In Table 2 the values of these terms are presented for six special moments during the tidal cycle: HW, LW, HWS, LWS, and for the tidal average situations (TA) during ebb and flood, respectively. In this table, it is assumed that the functions $\Psi$ and $\Phi$ behave like sinusoids, at least close to the points of HWS and LWS where this is relevant.

**Table 2.** Values of Terms Determining Tidal Propagation for HW, HWS, LW, LWS, and TA Situations

| | HW | LW | HWS | LWS | TA Ebb | TA Flood |
|---|---|---|---|---|---|---|
| $\xi$ | 0 | $\pi$ | $\varepsilon$ | $\pi + \varepsilon$ | $\pi/2$ | $3\pi/2$ |
| $\Phi$ | $\sin\varepsilon$ | $-\sin\varepsilon$ | 0 | 0 | $-\cos\varepsilon$ | $\cos\varepsilon$ |
| $\Phi'$ | $-\cos\varepsilon$ | $\cos\varepsilon$ | $-1$ | 1 | $-\sin\varepsilon$ | $\sin\varepsilon$ |
| $\Psi$ | 1 | $-1$ | $\cos\varepsilon$ | $-\cos\varepsilon$ | 0 | 0 |
| $C$ | $-\frac{c\tan\varepsilon}{\omega}\frac{1}{b}$ | $-\frac{c\tan\varepsilon}{\omega}\frac{1}{b}$ | 0 | 0 | $\frac{c}{\omega b\tan\varepsilon}$ | $\frac{c}{\omega b\tan\varepsilon}$ |
| $S$ | $-\frac{c\tan\varepsilon}{h_{HW}\omega}(I_b - I_r)$ | $-\frac{c\tan\varepsilon}{h_{LW}\omega}(I_b - I_r)$ | 0 | 0 | $\frac{c(I_b - I_r)}{\overline{h}\omega\tan\varepsilon}$ | $\frac{c(I_b - I_r)}{\overline{h}\omega\tan\varepsilon}$ |
| $R$ | $\frac{f\upsilon(\sin\varepsilon)^2}{h_{HW}\omega\cos\varepsilon}$ | $\frac{f\upsilon(\sin\varepsilon)^2}{h_{LW}\omega\cos\varepsilon}$ | 0 | 0 | $\frac{-f\upsilon\cos\varepsilon}{\overline{h}\omega}$ | $\frac{-f\upsilon\cos\varepsilon}{\overline{h}\omega}$ |
| $D_1$ | $\frac{g\eta\delta_H}{\upsilon\omega}\frac{1}{\cos\varepsilon}$ | $\frac{g\eta\delta_H}{\upsilon\omega}\frac{1}{\cos\varepsilon}$ | $\frac{g\eta\delta_H}{\upsilon\omega}\cos\varepsilon$ | $\frac{g\eta\delta_H}{\upsilon\omega}\cos\varepsilon$ | 0 | 0 |
| $D_2$ | $\frac{c\tan\varepsilon}{\omega}\delta_u$ | $\frac{c\tan\varepsilon}{\omega}\delta_u$ | 0 | 0 | $\frac{-c}{\omega\tan\varepsilon}\delta_u$ | $\frac{-c}{\omega\tan\varepsilon}\delta_u$ |
| $D_3$ | $\frac{c\tan\varepsilon}{h_{HW}\omega}\eta\delta_H$ | $-\frac{c\tan\varepsilon}{h_{LW}\omega}\eta\delta_H$ | 0 | 0 | 0 | 0 |
| $D_4$ | $\frac{\upsilon\sin\varepsilon\tan\varepsilon}{\omega}\delta_u$ | $-\frac{\upsilon\sin\varepsilon\tan\varepsilon}{\omega}\delta_u$ | 0 | 0 | $\frac{\upsilon\cos\varepsilon}{\omega\tan\varepsilon}\delta_u$ | $-\frac{\upsilon\cos\varepsilon}{\omega\tan\varepsilon}\delta_u$ |

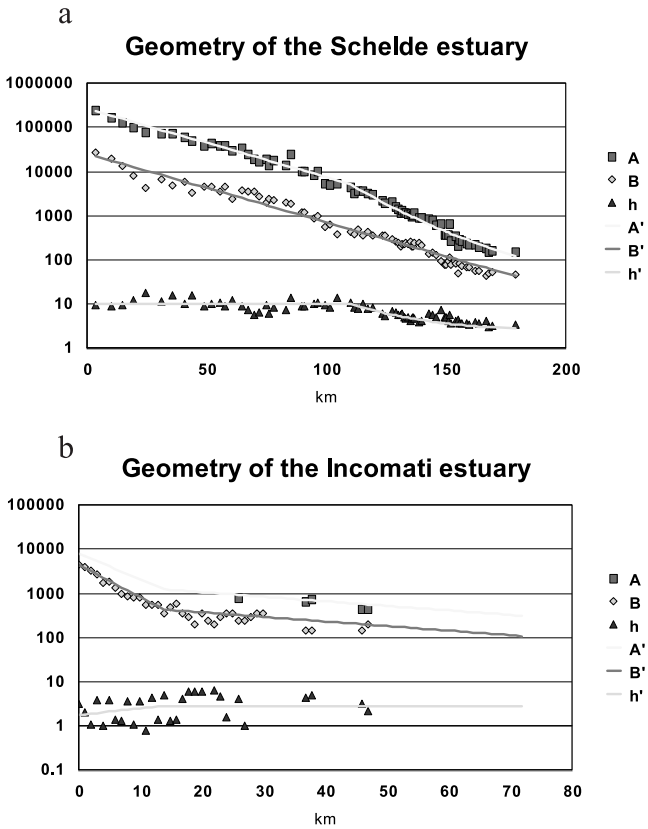


**Figure 4.** The geometry of the (a) Schelde estuary and (b) Incomati estuary, showing the longitudinal variation of the cross-sectional area in $m^2$ ($A$), the width in m ($B$) and the depth in m ($h$) at mean sea level. The accent indicates computed values. See color version of this figure in the HTML.

[37] If the tidal wave progresses as a nondeformed wave, any convenient moment during the tidal cycle can be selected to determine the wave celerity. It can be seen from Table 2 that it is very attractive to solve the equation for the moments of HWS and LWS where $v = 0$, $C = 0$, $S = 0$, $R = 0$, $D_2 = 0$, $D_3 = 0$, and $D_4 = 0$. Hence the equation for the celerity of the wave (at slack time) reads

$$c^2 = \frac{1}{\beta} gh \frac{1}{1-D} = \frac{c_0^2}{\left(1 - \frac{g}{\upsilon\omega}\frac{d\eta}{dx}\cos\varepsilon\right)}, \qquad (33)$$

where $D = D_1$ and $h$ is the water depth at slack time. Since the water depth at HWS is larger than at LWS, the celerity of the wave is slightly higher at HWS than at LWS. Hence the assumption that the wave is nondeformed is only valid if the depth at HWS is not much different from the depth at LWS, or if $\eta\cos\varepsilon \ll h$. In the latter case the average depth may be used.

[38] Equation (33) is an expansion of the classical equation for wave propagation by a simple damping factor $1/(1 - D)$. The equation obtained is surprisingly simple and provides clear insight into the factors that influence tidal propagation. It can be seen directly that the classical equation is obtained if convergence balances friction and there is no tidal damping or amplification. The wave is slowed down under tidal damping ($d\eta/dx < 0$) and accelerated under tidal amplification ($d\eta/dx > 0$).

[39] At TA, the depth is the same for the flood and ebb tide. The asymmetry between TA-flood and TA-ebb is in the $D_4$-term and in the left-hand member of equation (27) where the velocity has a different sign. Both cases of asymmetry are negligible if the Froude number is small. Disregarding the $D_4$-term, one can demonstrate that the celerity at TA and HWS/LWS is the same, making use of the equation for the tidal damping which was derived by *Savenije* [1998, 2001] from the full Saint Venant's equations. It is presented here without derivation:

$$\delta_H = \frac{1}{\eta}\frac{d\eta}{dx} = \frac{\left(\frac{1}{b} - f\frac{\upsilon\sin\varepsilon}{hc}\right)}{\left(1 + \frac{g\eta}{c\upsilon\sin\varepsilon}\right)} = \frac{\left(\frac{1}{b} - f\frac{\upsilon\sin\varepsilon}{hc}\right)}{\left(1 + \frac{1}{\alpha}\right)}. \qquad (34)$$

The first term in the numerator of this equation is the convergence term; the second term is the friction term. If friction prevails over convergence, the tidal wave is damped. Otherwise it is amplified. If the convergence term balances the friction term, there is no damping, in

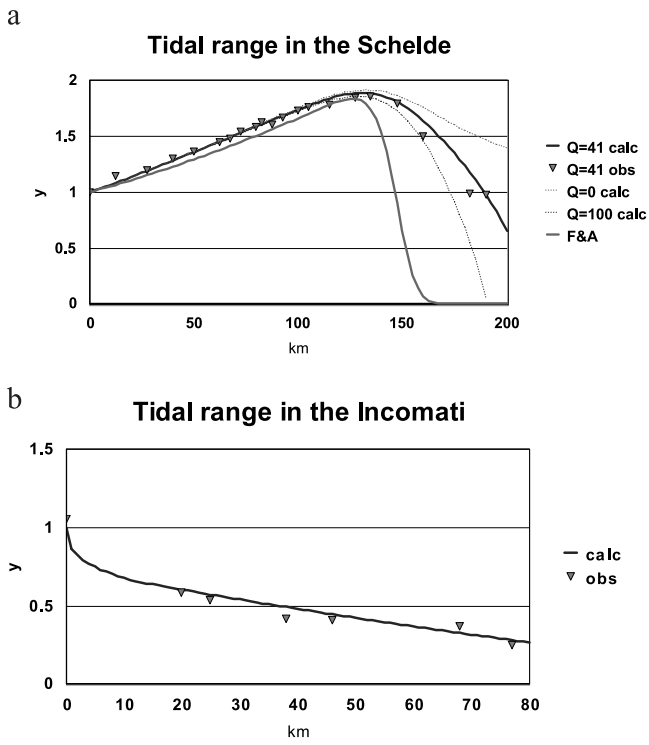


**Figure 5.** (a) Tidal damping in the Schelde estuary on 21 June 1995 (Q = 41 $m^3/s$) showing the dimensionless tidal range $y = H/H(0)$ against distance. The drawn line through the observations (triangles) and the dotted lines have been computed by *Horrevoets et al.* [2004] for different river discharges. The lower curve has been computed with the method of *Friedrichs and Aubrey* [1994]. (b) Tidal damping in the Incomati estuary on 30 July 1980 (Q = 4 $m^3/s$) showing the dimensionless tidal range $y = H/H(0)$ against distance. See color version of this figure in the HTML.

a

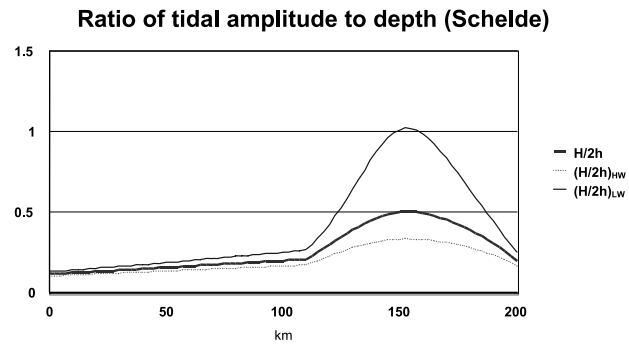


b

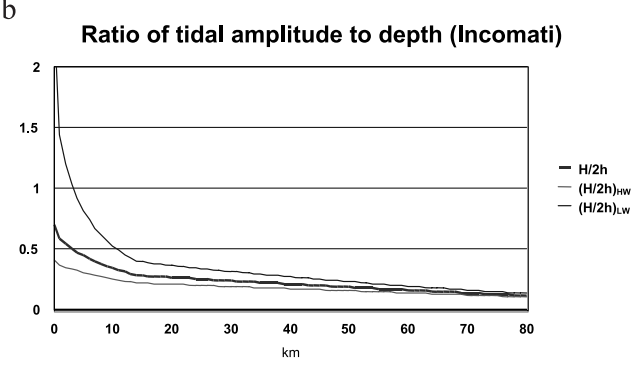


**Figure 6.** Ratio of tidal amplitude to depth $H/(2h)$ in the (a) Schelde estuary and (b) Incomati estuary. See color version of this figure in the HTML.

agreement with the concept of an ideal estuary. The denominator is an important term, since $\alpha$ is smaller than unity [*Savenije*, 2001]. By using (1) and (16), we can see that $\alpha \approx \sin^2\varepsilon$, which in the Schelde is about 0.1.

[40] In equation (33), the wave celerity can be computed on the basis of the observed damping of the tidal range. One can, however, also obtain an implicit expression for wave celerity by substitution of equation (34) in (33), resulting in

$$c^2 = \frac{1}{\beta} gh \frac{1}{1-D}$$

with

$$D = \frac{c \sin\varepsilon \cos\varepsilon}{\omega} \frac{\left(\frac{1}{b} - f\frac{\upsilon \sin\varepsilon}{hc}\right)}{(1+\alpha)} = \frac{\sin 2\varepsilon}{2(1+\alpha)}\left(\frac{c}{\omega b} - \frac{R'}{\omega}\right). \quad (35)$$

In equation (35), both the nominator and denominator of $D$ have been multiplied by $\alpha$. As a result, the denominator $(1+\alpha)$ has a value close to unity. In the right-hand side of equation (35) the friction term of *Jay* [1991] is used, with $R' = f\upsilon\sin\varepsilon/h$. For the convergence, *Jay* [1991] uses the parameter $\Delta l = c(b\omega)^{-1}$. It can be seen clearly that $c = c_0$ when these two terms are equal. This can also be seen in Jay's Figure 3, where the lines of equation (35) plot a similar pattern.

[41] A case of critical convergence occurs when $D$ approaches unity. *Jay* [1991] observed that this happens when flow resistance is neglected and the convergence term $\Delta l = 2$. In (35), critical convergence occurs when $\Delta l = 2(1+\alpha)/\sin(2\varepsilon)$, which is larger than 2.

[42] One can simplify (35) further by substitution of (15).

$$D = \frac{\cos^2\varepsilon}{(1-\delta b)} \frac{\left(1 - fb\frac{\upsilon \sin\varepsilon}{hc}\right)}{(1+\alpha)}. \quad (36)$$

Equation (36) shows that the damping term is determined by the phase lag $\varepsilon$ and the balance between convection and friction. It can also be seen that $D$ is always smaller than unity and that critical convergence does not occur. (The only factor that can make $D$ larger than unity is $(1 - \delta b)$ under tidal amplification. In the Schelde, this term can reach a minimum value of 0.82, while $\cos^2\varepsilon = 0.89$ and $(1 + \alpha) = 1.11$). Furthermore, we see the crucial role of $\varepsilon$ in tidal wave propagation, as the key parameter determining the deviation of the wave celerity from $c_0$. If $\varepsilon = 0$: $D = 1$ and $c \to \infty$; if $\varepsilon = \pi/2$: $D = 0$ and $c = c_0$.

## 3. Empirical Verification in the Schelde and Incomati Estuaries

[43] The theory described in the previous section has been confronted with observations made in the Schelde and Incomati estuaries. Figures 4a and 4b show the geometry of these estuaries, where the cross-sectional area, the width, and the depth are plotted on semi-logarithmic paper. It can be seen that indeed the width and the cross-sectional area vary

a

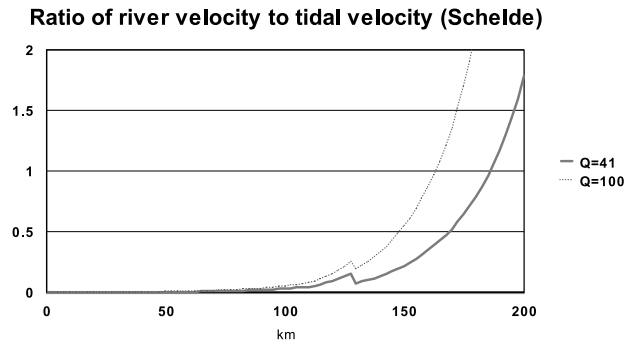


b

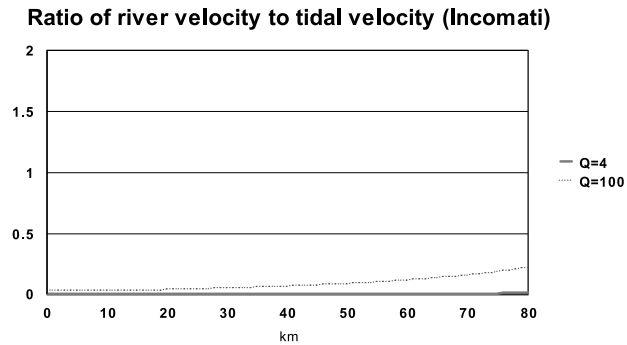


**Figure 7.** (a) Ratio of the velocity of the river discharge to the tidal velocity in the Schelde estuary for a river discharge of 41 $m^3/s$ (solid line) and 100 $m^3/s$ (dotted line). (b) Ratio of the velocity of the river discharge to the tidal velocity in the Incomati estuary for a river discharge of 4 $m^3/s$ (solid line) and 100 $m^3/s$ (dotted line). See color version of this figure in the HTML.

a

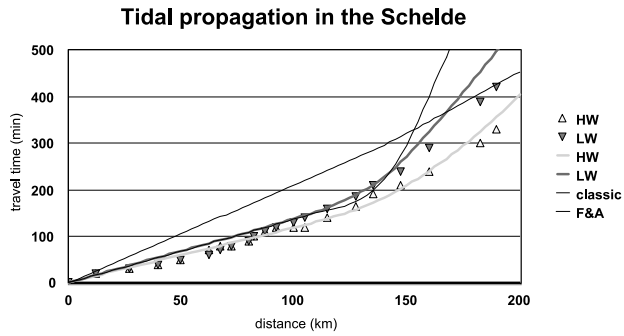


b

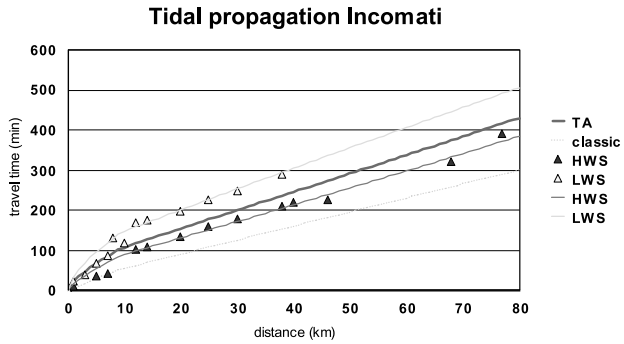


**Figure 8.** (a) Propagation of the tidal wave in the Schelde estuary observed at high water (HW) and low water (LW) 21 June 1995 (indicated by triangles). The thick solid lines represent the computed wave propagation at HW and LW. The dotted line represents the classical wave propagation. The thin solid line represents the wave propagation according to the method of *Friedrichs and Aubrey* [1994]. (b) Propagation of the tidal wave in the Incomati estuary at high water slack (HWS) and low water slack (LWS) observed on 23 June 1993 (indicated by triangles). The solid lines represent the computed wave propagation at HWS, LWS (thin solid lines) and mean tide (thick solid line). The dotted line represents the classical wave propagation. See color version of this figure in the HTML.

as exponential functions and that there is no significant bottom slope. Only in the upper end of the Schelde, where the estuary gradually becomes riverine in character, we see the Schelde estuary becoming shallow. The Schelde appears to have an average depth of 10.5 m and a convergence length of 28 km. The Incomati has two branches of the exponential function. In the lower part the convergence length is 6 km, and in the upper part it is 42 km. The average depth is 2.9 m.

[44] In Figure 5 the observed variation of the tidal range along the estuary axis in the Schelde and Incomati is shown. In Figure 5a, the lines indicating a river discharge of 41 and 100 $m^3/s$ were computed by *Horrevoets et al.* [2004]; the line with no river discharge corresponds with equation (34). The line indicated by F&A has been obtained with the method of *Friedrichs and Aubrey* [1994]; the deviation from the observed values is largely due to the high tidal amplitude to depth ratio in this part of the estuary. One can clearly see the strong amplification of the tidal range in the Schelde over the lower 130 km, after which the wave is damped. Figure 5b shows similar graphs for the Incomati with a discharge of 4 $m^3/s$. The Incomati experiences tidal damping throughout. In this estuary the method of Friedrichs and Aubrey could not be applied owing to the high value of the tidal amplitude to depth ratio near the estuary mouth.

[45] In Figure 6 the ratio of the tidal amplitude to depth is shown for the two estuaries, distinguishing between HW, LW, and mean tide (TA). It can be seen that the condition that this ratio should be less than unity is violated during low water near the mouth of the Incomati and around 150 km from the mouth in the Schelde. At these locations the assumptions made for the derivation are not justified and deviations are expected. Figure 7 presents the ratio of the velocity of the river discharge to the tidal velocity amplitude for the Schelde and Incomati. Figure 7a presents the lines for a discharge of 41 $m^3/s$, which occurred on 21 June 1993, and a line for a high discharge. It can be seen that the condition that the effect of river discharge is negligible does not apply in the upper part of the estuary. In the Incomati the effect of river discharge is negligible for the period of observation, and for a higher discharge of 100 $m^3/s$ as well.

[46] Figure 8 shows the application of the theory to wave celerity in the two estuaries. The new equation performs considerably better than the classical equation. In the Incomati the correspondence is very good, with the exception of the part nearest to the mouth. In the Schelde the line for HW is very good, but the line for LW shows a deviation upstream from the point located 150 km from the mouth. The reasons for these deviations should be sought in the relatively high ratio of tidal amplitude to depth and the effect of river discharge (see Figures 6a and 7a). As a comparison, Figure 8a also show the relation derived by *Friedrichs and Aubrey* [1994] for the tidal average situation.

[47] Figure 9a shows the variation of the damping term $D$ as a function of $x$ in the Schelde estuary. The thick line is the value obtained by (33) using observed values of $d\eta/dx$. The line indicated by $D$ is obtained with (35). The reason why this line deviates from the previous line upstream from 140 km is because it does not take into account the effect of river discharge on tidal damping. This can be seen if we consider the thin line (indicated by $D'$), which was obtained by using a slightly more sophisticated formula than (34), developed by *Horrevoets et al.* [2004] taking into account the effect of river discharge. This line fits the observed equation very well. Finally, the line indicated by $D''$ is the one using (36) which makes use of (15). The latter equation is more sensitive to a high river flow and amplitude to depth ratio. However, it can be seen that equation (36) is a good approximation for the tide-dominated part of the Schelde estuary. In the Incomati, where the river discharge is very small, we see that all curves except $D''$ are close. The latter is not appropriate near the estuary mouth where the tidal amplitude to depth ratio is large.

## 4. Conclusion

[48] One can conclude that the new equation is a substantial improvement over the classical equation for tidal wave propagation and that new insight has been gained into the propagation of tidal waves under damped or amplified conditions. Equations (33)–(36) are the result of an integrated theory for wave celerity and wave attenuation. The wave celerity and the tidal damping both depend on the balance between friction and convergence. If convergence is

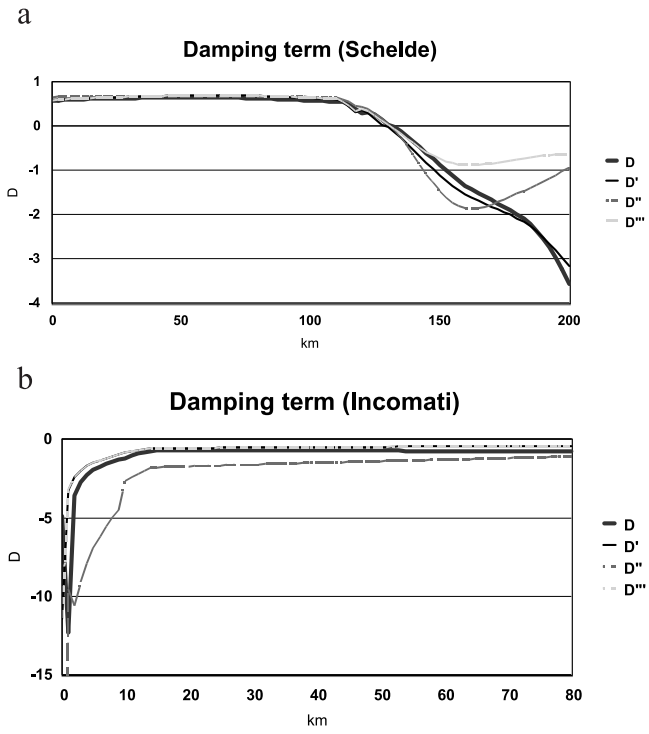


**Figure 9.** The variation of the damping term along the axis of the (a) Schelde estuary and (b) Incomati estuary. $D$ indicates the damping term obtained by equation (28), using observed values of $d\eta/dx$. $D'''$ was obtained with equation (30), $D''$ with equation (31), and $D'$ by using the equation of *Horrevoets et al*. [2004] that accounts for the effect of river discharge on tidal damping. See color version of this figure in the HTML.

stronger than friction, the tidal wave is amplified and the celerity of the wave is larger than $c_0$; if friction is stronger than convergence, the tidal wave is damped and the wave celerity is slower than $c_0$. The phase lag $\varepsilon$ is a crucial parameter to describe tidal wave propagation in estuaries.

## Notation

$A$ cross-sectional area, $L^2$, where L is length unit.
$b$ convergence length of the stream width, L.
$B$ stream width, L.
$B_s$ storage width, L.
$B_0$ width at the estuary mouth, L.
$c$ wave celerity, L/T, where T is time unit.
$c_0$ classical wave celerity, L/T.
$C$ convergence term.
$D$ damping term.
$f$ roughness coefficient.
$F$ damping parameter.
$g$ acceleration due to gravity, $L/T^2$.
$h$ stream depth, L.
$H$ tidal range, L.
$I_r$ density slope.
$I_b$ bottom slope.
$Q$ discharge, $L^3/T$.
$Q_r$ river discharge, $L^3/T$.
$R$ friction term.
$S$ slope term.
$t$ time, T.
$T$ tidal period, T.
$v$ flow velocity (averaged over the cross-section), L/T.
$x$ distance, L.
$y$ dimensionless tidal range $H/H(0)$.
$z$ side slope.
$z_b$ bottom elevation, L.
$\alpha$ constant.
$\beta$ storage width correction factor.
$\delta_H$ damping scale of tidal range, $L^{-1}$.
$\delta_u$ damping scale of tidal velocity amplitude, $L^{-1}$.
$\varepsilon$ phase lag between HW and HWS, or LW and LWS.
$\xi$ dimensionless argument.
$\rho$ density of the water, $ML^{-3}$.
$\upsilon$ tidal velocity amplitude, L/T.
$\omega$ angular velocity, $T^{-1}$.
$\Phi$ harmonic function of the tidal velocity.
$\Psi$ harmonic function of the water level.

[49] **Acknowledgment.** The authors would like to acknowledge two anonymous reviewers and D. A. Jay for very useful comments and suggestions.

## References

Airy, G. B. (1845), *Tides and Waves, Encyc. Metropol.*, vol. 5, pp. 241–396, Gale and Fenner, London.
Dronkers, J. J. (1964), *Tidal Computations in Rivers and Coastal Waters*, Elsevier, New York.
Friedrichs, C. T., and D. G. Aubrey (1994), Tidal propagation in strongly convergent channels, *J. Geophys. Res.*, *99*(C2), 3321–3336.
Godin, G. (1991), Frictional effects in river tides, in *Tidal Hydrodynamics*, edited by B. B. Parker, pp. 379–402, John Wiley, Hoboken, N. J.
Godin, G. (1999), The propagation of tides up rivers with special considerations on the upper Saint Lawrence river, *Estuarine Coastal Shelf Sci.*, *48*, 307–324.
Harleman, D. R. F. (1966), Tidal dynamics in estuaries part II: Real estuaries, in *Estuary and Coastline Hydrodynamics*, edited by A. T. Ippen et al., pp. 493–545, McGraw-Hill, New York.
Horrevoets, A. C., H. H. G. Savenije, J. N. Schuurman, and S. Graas (2004), The influence of river discharge on tidal damping in alluvial estuaries, *J. Hydrol.*, *294*, 213–228.
Hunt, J. N. (1964), Tidal oscillations in estuaries, *Geophys. J. R. Astron. Soc.*, *8*, 440–455.
Jay, D. A. (1991), Green's law revisited: Tidal long-wave propagation in channels with strong topography, *J. Geophys. Res.*, *96*(C11), 20,585–20,598.
Lamb, H. (1932), *Hydrodynamics*, Cambridge Univ. Press, New York.
Lanzoni, S., and G. Seminara (1998), On tide propagation in convergent estuaries, *J. Geophys. Res.*, *103*(C13), 30,793–30,812.
Lanzoni, S., and G. Seminara (2002), Long-term evolution and morphodynamic equilibrium of tidal channels, *J. Geophys. Res.*, *107*(C1), 3001, doi:10.1029/2000JC000468.
Pillsbury, G. (1939), *Tidal Hydraulics*, U.S. Corps of Eng., Vicksburg, Va.
Ponce, V. M., and D. B. Simons (1977), Shallow wave propagation in open channel flow, *J. Hydraul. Div.*, *103*(HY12), 1461–1476.
Prandle, D. (2003), Relationships between tidal dynamics and bathymetry in strongly convergent estuaries, *J. Phys. Oceanogr.*, *33*, 2738–2750.
Savenije, H. H. G. (1992), Lagrangean solution of St. Venant's equations for an alluvial estuary, *J. Hydraul. Eng.*, *118*(8), 1153–1163.
Savenije, H. H. G. (1993), Determination of estuary parameters on the basis of Lagrangian analysis, *J. Hydraul. Eng.*, *119*(5), 628–643.
Savenije, H. H. G. (1998), Analytical expression for tidal damping in alluvial estuaries, *J. Hydraul. Eng.*, *124*(6), 615–618.
Savenije, H. H. G. (2001), A simple analytical expression to describe tidal damping or amplification, *J. Hydrol.*, *243*(3–4), 205–215.
Sobey, J. (2001), Evaluation of numerical models of flood and tide propagation in channels, *J. Hydraul. Eng.*, *127*(10), 805–824.
Whitham, G. B. (1974), *Linear and Nonlinear Waves*, John Wiley, Hoboken, N. J.

H. H. G. Savenije and E. J. M. Veling, Delft University of Technology, P.O. Box 5048, Delft, NE-2600 GA, Netherlands. (h.h.g.savenije@citg.tudelft.nl)